

Ripple-Free Phase-Pole Modulation of a Multiphase Induction Machine

Omer Ikram ul Haq
Dept. Energy Conversion
ABB Corporate Research
Västerås, Sweden
omer.ikramulhaq@se.abb.com

R. S. Kanchan
Dept. Energy Conversion
ABB Corporate Research
Västerås, Sweden
rahul.kanchan@se.abb.com

Luca Peretti
Div. of Electric Power and Energy Systems
KTH Royal Institute of Technology
Stockholm, Sweden
lucap@kth.se

Sjoerd G. Bosga
Dept. Energy Conversion
ABB Corporate Research
Västerås, Sweden
sjoerd.bosga@se.abb.com

Abstract: A multiphase induction machine model using vector space decomposition provides insights into many space harmonics through decoupled reference frames. These decoupled reference frames host specific space vectors related to particular space harmonics. Based on the physical winding configuration, these vector spaces can be excited independently or simultaneously for the production of torque. Each torque-producing vector space generates a unique number of magnetic pole pairs and has independent torque-slip characteristics. In most literature, the transition between these magnetic pole pairs is achieved by magnetizing a desired vector space and then performing the torque transition. This approach results in beat oscillations due to interference between magnetized vector spaces. This paper proposes a solution that eliminates these beat oscillations during magnetic pole-pair transition while optimizing the stator current peaks. The effectiveness of this synchronized phase-pole modulation solution is experimentally verified on a 9-phase induction machine in comparison to the standard magnetic pole-pair transition methods.

Index Terms—multiphase electric machines, online phase-pole transition, inter plane magnetic cross coupling

I. INTRODUCTION

Multiphase electrical machines (MPEMs) are becoming more and more present in drive applications [1], [2]. They have the potential for higher torque and power density [3] and are inherently fault tolerant under certain conditions [4]. These unique properties of MPEMs make them suitable for applications such as aerospace [5], marine propulsion [6], electric generators [7] and electric vehicles [8]. A special category of MPEMs, i.e phase-pole modulating induction machines (PPMIMs), allows changing the number of magnetic pole pairs without any hardware reconfiguration [9], [10]. To achieve this, the physical winding of the MPEM can be

configured in many ways, and the choice is crucial [11]–[13]. Winding types are categorized into symmetrical winding (SW) and asymmetrical winding (ASW) configurations [14]. Multiple vector spaces can be controlled depending on the choice of winding configuration. These vector spaces are composed of multiple space harmonics [9], [15] which are independent within the linear region of the MPEM. Current in each vector space generates a unique number of magnetic pole-pairs [9], thus having a unique torque-slip characteristic. These decomposed vector spaces can be excited simultaneously to produce additive torques [9], increasing the torque density, or transitioning between them to access a unique torque-slip characteristic [10], [16]–[19], extending the operating range of the MPEM. However, due to the interaction between magnetic flux produced by different vector spaces in the non-linear region (saturated core) of the MPEM, the pole transition generates significant torque ripples. This phenomenon is mainly due to inter-plane cross-coupling (IPXC) [20]. IPXC is the magnetic cross-coupling between transitioned vector spaces due to the saturation of the shared stator and rotor iron core. Furthermore, the interaction between vector spaces during transition produces interference patterns resulting in amplitude modulation at a beat frequency on the MPEM’s electrical quantities. This destructive and constructive interference of rotor flux is observed as torque ripples at the shaft of the MPEM. In order to avoid the adverse effects of IPXC and beat frequency oscillations, [3] provides a generic solution by distributing the torque reference in between different vector spaces such that the slip frequencies of different vector spaces are controlled with unique relationship. [3] also provides a generalised phase relationship between different vector spaces which will minimize the peak amplitudes of a given space vector I_s and ψ_r . However, the proposed solution is not capable of performing a magnetic pole change. This paper builds upon the state-of-the-art established by [3] and introduces the capability of pole transition while minimizing the stator current peaks. The proposed improvements are experimentally

validated using a 9-phase induction machine (IM) laboratory setup, and the results are compared with earlier results using pole pair transition approach described in [10].

II. MULTIPHASE INDUCTION MACHINE MODEL

SW and ASW configurations of a MPEM can be modeled using either vector-space decomposition (VSD) or harmonic plane decomposition (HPD) [10]. However, in this paper VSD is used for modeling a given MPEM. The VSD transforms the space-vector quantities from the fundamental 123 reference frame [21] to the stationary $\alpha\beta\gamma$ reference frame as follows:

$$\mathbf{x}_{\alpha\beta\gamma} = \underbrace{\left(\frac{2}{m}\right)^K \mathbf{C}_s}_{\mathbf{T}_{123 \rightarrow \alpha\beta\gamma}} \cdot \mathbf{x}_{123}; \quad \mathbf{x}_{123} = \underbrace{\left(\frac{2}{m}\right)^{1-K} \mathbf{C}_s^T}_{\mathbf{T}_{\alpha\beta\gamma \rightarrow 123}} \cdot \mathbf{x}_{\alpha\beta\gamma} \quad (1)$$

$$\mathbf{C}_s = \begin{bmatrix} 1 & \cos(1\delta) & \cos(2\delta) & \dots & \cos((m-1)\delta) \\ 0 & \sin(1\delta) & \sin(2\delta) & \dots & \sin((m-1)\delta) \\ 1 & \cos(3\delta) & \cos(6\delta) & \dots & \cos((m-1)3\delta) \\ 0 & \sin(3\delta) & \sin(6\delta) & \dots & \sin((m-1)3\delta) \\ \vdots & \vdots & \vdots & \ddots & \vdots \\ 1 & \cos(\xi\delta) & \cos(2\xi\delta) & \dots & \cos((m-1)\xi\delta) \\ 0 & \sin(\xi\delta) & \sin(2\xi\delta) & \dots & \sin((m-1)\xi\delta) \end{bmatrix}$$

$$\delta = \frac{\pi}{m}; \quad \xi = \begin{cases} m & \text{if } m \text{ odd} \\ m-1 & \text{if } m \text{ even} \end{cases}$$

In (1), $K = 1$ for amplitude-invariant transformations, while $K = 0.5$ for power-invariant transformations, and δ is the angle between each magnetic phasor represented in half-wave symmetry [14]. This $\alpha\beta\gamma$ transformation decouples the space harmonic contents of the space-vector quantity distribution along the stator circumference, including a homopolar component (i.e. γ) for an odd number of phases, which is not considered in this paper and set to zero. Furthermore, the MPEM is assumed to be magnetically balanced reducing the even vector spaces to zero [9]. Thus, only odd vector spaces are available, i.e. $\nu \in \{1, 3, 5, \dots, \xi\}$, where ξ is the largest odd number less than or equal to the total number of phases (i.e. m). These vector spaces are independent under the condition that the MPEM is not magnetically saturated.

A generalized Park transformation brings the space-vector quantities from the $\alpha\beta$ reference frame to the rotating dq reference frame. Leveraging the independence of the vector spaces allows to apply a rotational transformation to each of the space vectors independently. This rotational reference frame is defined by $\phi_s^{(\nu)}$, and the resulting Park transformation matrix is given by

$$\mathbf{T}_{\alpha\beta \rightarrow dq} = \begin{bmatrix} \cos\left(\phi_s^{(\nu)}\right) & -\sin\left(\phi_s^{(\nu)}\right) \\ \sin\left(\phi_s^{(\nu)}\right) & \cos\left(\phi_s^{(\nu)}\right) \end{bmatrix} \quad (2)$$

Thus, the machine model in each vector space resembles the one for the conventional three-phase machine, shown in Fig. 1 and described by (3), which is given in the rotor flux (i.e. $\psi_r^{(\nu)}$) reference frame.

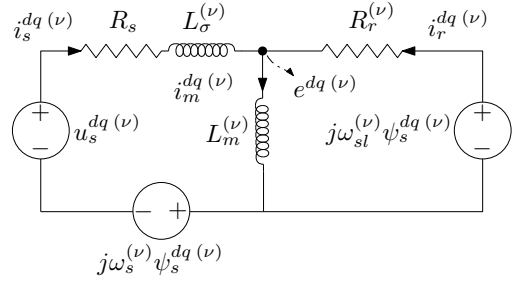


Fig. 1. Inverse- Γ equivalent circuit of vector space ν .

$$u_s^{dq(\nu)} = i_s^{dq(\nu)} R_s^{(\nu)} + \frac{d}{dt} \psi_s^{dq(\nu)} + j\omega_s^{(\nu)} \psi_s^{dq(\nu)} \quad (3)$$

$$0 = i_r^{dq(\nu)} R_r^{(\nu)} + \frac{d}{dt} \psi_r^{dq(\nu)} + j\omega_{sl}^{(\nu)} \psi_r^{dq(\nu)}$$

where

$$\omega_{sl}^{(\nu)} = \omega_s^{(\nu)} - \omega_r^{(\nu)} \quad (4)$$

and

$$\psi_s^{dq(\nu)} = i_s^{dq(\nu)} L_s^{(\nu)} + L_m^{(\nu)} (i_s^{dq(\nu)} + i_r^{dq(\nu)}) \quad (5)$$

$$\psi_r^{dq(\nu)} = L_m^{(\nu)} (i_s^{dq(\nu)} + i_r^{dq(\nu)})$$

III. MAGNETIC POLE-PAIR TRANSITION (MPT) BETWEEN DECOMPOSED VECTOR SPACES

Depending upon the winding configuration, few of these decomposed vector spaces can produce useful torque [9]. Each of these torque-producing vector spaces generates unique numbers of magnetic pole pairs given by $p^{(\nu)} = \nu \cdot p^{(1)}$ [9], where $p^{(\nu)}$ is the number of magnetic pole-pairs generated by vector space ν , and $p^{(1)}$ is the number of pole-pairs generated by the fundamental vector space. As an example, lab measurement of $1 \rightarrow 3$ MPT is shown in Fig. 2 implementing the asynchronous MPT technique proposed in [10]. The MPT is handled by a state machine that manipulates the $i_s^{dq(\nu)*}$ in order to achieve pole pair transition. Here the superscript “*” corresponds to the reference quantities. The function of MPT’s state-machine is divided into three steps:

- Step 1:** Pre-magnetizing of vector space 3 by increasing $i_s^{d(3)}$.
- Step 2:** Transferring torque from vector space 1 to vector space 3 by reducing $i_s^{d(1)}$ and increasing $i_s^{d(3)}$.
- Step 3:** Demagnetizing vector space 1 by reducing $i_s^{d(1)}$ to zero.

During Step 1, significant torque ripples are observed. This is mainly due to the constructive and destructive interference of two magnetic fields (i.e. 1 and 3 vector space), saturating and de-saturating the iron core with a beat frequency [3]. This results in the fluctuations in the parameter of the PPMIM resulting in torque oscillations. However, during Step 3 the impact of interference is negligible. The reduction in the large magnetic field component in vector space 1 causes the core to de-saturate, thereby reducing the torque ripples.

Similarly, the amplitude of the stator current is modulated with the beat oscillations due to constructive and destructive interference between the currents of vector space 1 and 3.

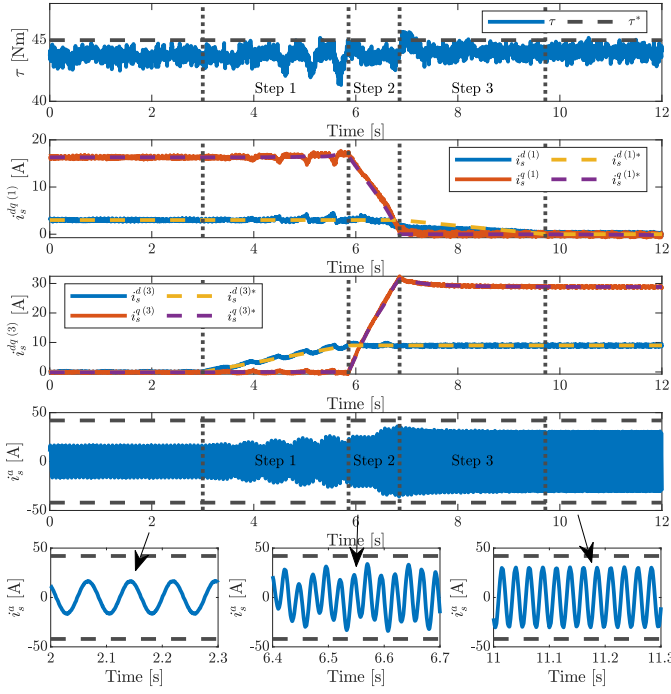


Fig. 2. Asynchronous 1 → 3 MPT technique

This interference results in current peaks risking an over-current fault and increase losses. The same phenomenon can be observed in stator voltage which might trigger field-weakening of the PPMIM. All of these phenomena are undesired and can be avoided by applying proposed ripple free pole-pair transition (RFPT).

IV. RIPPLE-FREE POLE-PAIR TRANSITION (RPFT) USING SMOOTH REFERENCE FRAME TRANSITION (SRFT)

The beat oscillations due to non-synchronous vector spaces as explained in [3]. They can be avoided by synchronizing the slip frequencies (i.e. $\omega_{sl}^{(\nu)}$) of each vector space as given by

$$\omega_{sl}^{(1)} = \frac{\omega_{sl}^{(3)}}{3} = \dots = \frac{\omega_{sl}^{(\xi)}}{\xi} \quad (6)$$

This synchronization is achieved by distributing the torque reference (i.e. τ^*) between the vector spaces to be synchronously transitioned. The amount of torque distribution is a function of rotor flux linkage ($\psi_r^{(\nu)}$) and is given by

$$\tau^{(\nu)*} = \kappa^{(\nu)} \tau^* \quad (7)$$

where,

$$\kappa^{(\nu)} = \frac{(\nu\psi_r^{(\nu)})^2}{R_r^{(\nu)}} \left(\sum_{x=1,3,5,\dots}^{\xi} \frac{(x\psi_r^{(x)})^2}{R_r^{(x)}} \right)^{-1} \quad (8)$$

However, the control topology proposed in [3] requires a master vector space whose rotor flux vector is used for reconstructing the reference frames for the rest of the available vector spaces, and thus can not be demagnetized. This paper

improves upon the given control topology and implements torque sharing driven by (7) and combines it with modified MPT proposed in [10]. This combination of torque sharing and MPT is terms as RFPT. Furthermore, the smooth reference frame transition (SRFT) reconstructs the reference frame for each vector space by combining the reference frames of active vector spaces thus, eliminating the need for a master vector space. This is achieved by a weighted transition between normalized slip frequencies (i.e. $\omega_{slm}^{(\nu)}$) of active vector spaces and is given by

$$\hat{\omega}_{slm} = \frac{\sum_{x=1,3,\dots}^{\xi} \hat{\omega}_{slm}^{(x)} i_s^{d(x)*}}{\sum_{x=1,3,\dots}^{\xi} i_s^{d(x)*}} \quad (9)$$

where

$$\hat{\omega}_{slm}^{(x)} = \frac{\hat{\omega}_{sl}^{(x)}}{p^{(x)}} \quad (10)$$

The quantities with “^” are the estimated quantities obtained from the flux observer described in [22]. Using $\hat{\omega}_{slm}$, the stator frequencies i.e. $\hat{\omega}_s^{(\nu)}$ and transformation angle i.e. $\hat{\phi}_s^{(\nu)}$ of each vector space is calculated by

$$\hat{\omega}_s^{(\nu)} = (\omega_m + \hat{\omega}_{slm}) p^{(\nu)} \quad (11)$$

$$\hat{\phi}_s^{(\nu)} = \int \hat{\omega}_s^{(\nu)} dt \quad (12)$$

A control block diagram implementing the proposed RFPT for a PPMIM having ξ vector spaces is shown in Fig.3, while the implementation of SRFT is shown in Fig. 4. In Fig.3, “CC & FF” implements simple PI current controllers (CC) and feed-forward (FF) based on (3), taking care of the decoupling between d and q axes of each vector space. The “ $\psi_r^{(\nu)}$ Observer” constructs the rotor flux vector $\hat{\psi}_r^{(\nu)}$ and estimates the slip frequencies $\hat{\omega}_{sl}^{(\nu)}$ explained in [22] for a standard IM. The proposed MPT is achieved by changing the magnetization level of the vector spaces to be transitioned. This transition is handled by RFPT state machine shown in Fig. 5. The input to the state machine is the desired number of pole pairs (i.e. $p^* \in \{1, 3, \dots, \xi\}$). At the startup, this p^* is set to a default value (i.e. p^d) which defines the initial pole pair configuration of the state machine. When a new pole pair configuration is requested, the state machine first ramps up the $i_s^{d(\nu)}$ of the corresponding vector space to a nominal level (i.e. $i_s^{d(\nu)n}$). Once the $i_s^{d(\nu)}$ reaches steady-state, all other vector spaces are demagnetized by reducing their i_s^d to zero. During this whole procedure, the $\tau^{(\nu)*}$ is defined by (7) achieving a RFPT.

Finally, the peak optimization of a resultant vector quantity of PPMIM e.g. stator current (i_s), stator voltage (u_s), stator flux linkage (ψ_s), or rotor flux linkage (ψ_r) is implemented as explained in section IV-A of [3]. This resultant vector quantity is the geometrical sum of all active space vectors. At a time, only one resultant vector can be optimized, and the choice is

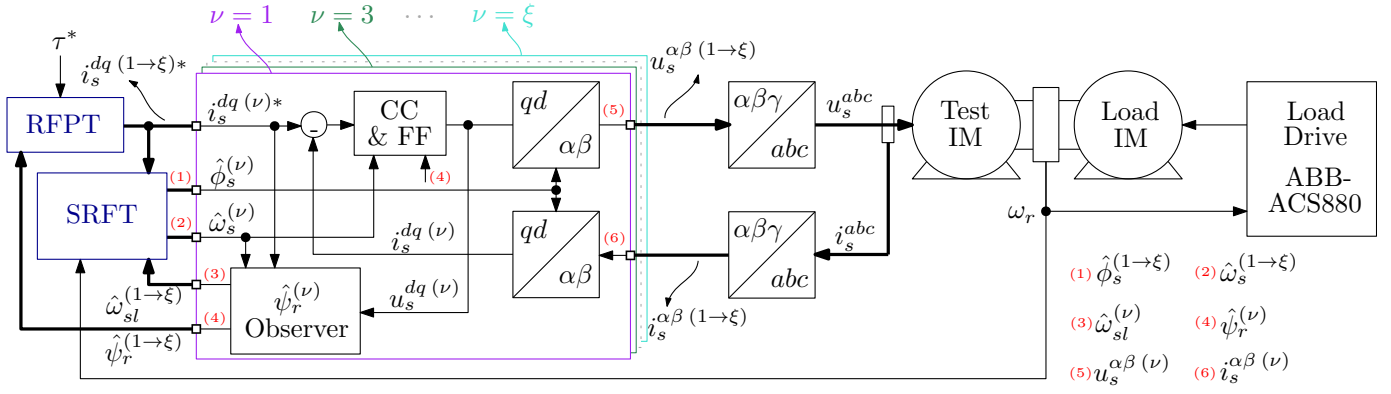


Fig. 3. Overview control topology for ripple-free magnetic pole-pair transition (RFPT)

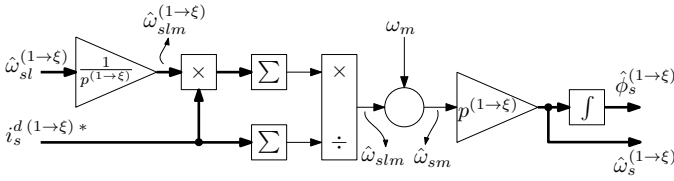


Fig. 4. Proposed control block diagram SRFT.

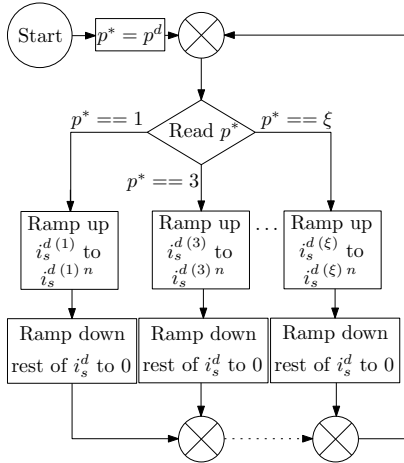


Fig. 5. Flow chart of RFPT state-machine

dependent on PPMIM's operating point. In this paper, only the peak optimization of the resultant stator current will be demonstrated during RFPT, which is valid for other vectors as well.

V. EXPERIMENTAL VALIDATION

The above-proposed method of ripple-free magnetic pole transition of a PPMIM using SRFT is evaluated on an experimental setup consisting of a 9-phase IM drive.

A. Experimental Setup

The experimental test setup, shown in Fig. 6, consists of four 3-phase converters (i.e., C1, C2, C3, and C4) controlled by a real-time controller (Opal-RT OP5700). These converters have

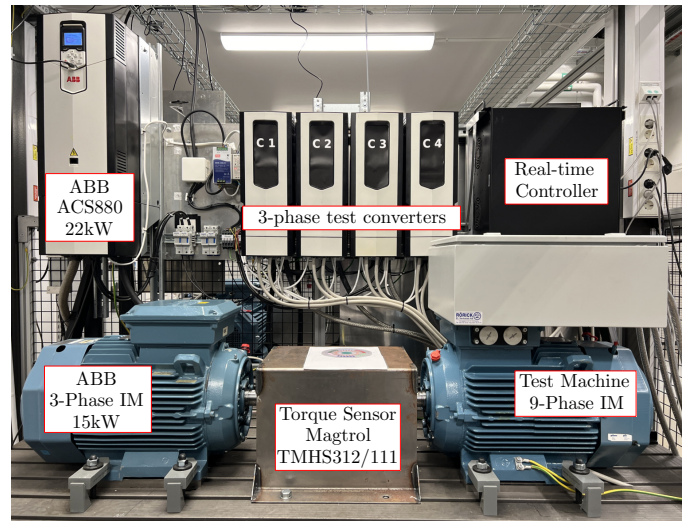


Fig. 6. PPMIM experimental test bench.

a common DC-link voltage powered by a 22 kW regenerative load drive (ABB ACS880). The load drive also controls a 15 kW 3-phase 1 pole-pair IM which is mechanically coupled to the test machine. Furthermore, the controller is interfaced with a 1000-pulse encoder and a torque transducer to measure rotor speed and output torque.

The test machine [23], which was a standard three-phase induction machine with 36 stator slots and 28 rotor bars, is retrofitted with the individual coils to form a multiphase winding set of different pole-phase pair combinations. The stator winding is composed of 18 coils (i.e., open-end distributed winding, full-pitched single slot machine coils) with a return path shifted by 180° mechanical degrees. This type of coil distribution provides the freedom to physically configure the windings into 3, 6, and 9-phase arrangements producing a fundamental magnetic field of 1 pole pair as discussed in [23].

To evaluate the proposed concepts in this paper, this test machine is configured as a 9-phase SW IM, requiring only three 3-phase converters. The SW configuration is chosen due to the advantage of more usable vector spaces of a 9-phase

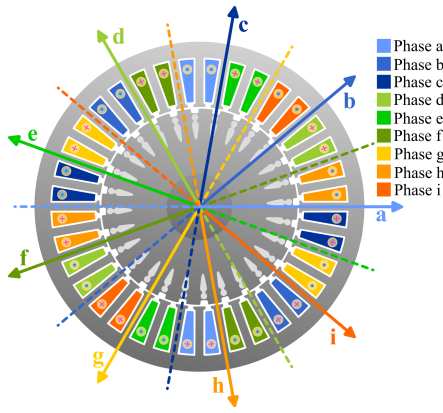


Fig. 7. Coil connections of the open-end distributed winding for the 9-phase symmetrical windings.

TABLE I
MEASURED ELECTRICAL PARAMETERS (INVERSE- Γ) OF THE TEST MACHINE CONFIGURED AS 9-PHASE SW.

ν	R_s [m Ω]	L_{σ} [mH]	L_m [mH]	R_r [m Ω]
1	285	7.3	175.8	192.6
3	285	5.0	17.4	106.8
5	285	3.9	4.8	67.4
7	285	3.1	2.0	45.5

SW machine [9]. Fig. 7 shows the coil connections of the test machine for the 9-phase SW arrangement, and its fundamental and higher order vector space equivalent circuit parameters are given in TABLE I. These parameters are obtained using an offline parameter estimation method for multiphase induction machines elaborated in [23].

B. Experimental evaluation of proposed RFPT

The two methods (i.e. asynchronous method [10], [16] and proposed RFPT method) of MPT are evaluated on the laboratory test bench described in the section V-A. The asynchronous method implements the control strategy explained in [10], [16], while the proposed method implements the control topology based on RFPT shown in Fig. 3 for 1 \leftrightarrow 3 MPT. The laboratory measurements for both methods are taken under similar conditions i.e. the torque reference $\tau^* = 45$ Nm and rotor speed $n_r = 800$ rpm. Furthermore, during these tests, the load machine is operated in speed-control mode, while the test machine is controlled in torque-control mode. Fig. 2 shows the laboratory measurement result of the asynchronous method which will be used as a benchmark, while the experimental result obtained with the proposed method is shown in Fig. 8. In contrast to the prior art method, the proposed method transitions from vector space 1 to vector space 3 just in two steps defined in RFPT's state machine. These steps are:

Step 1: Vector space 3 is magnetized by increasing $i_s^{d(3)}$ while $i_s^{d(1)}$ is kept constant. Based on the magnitude of $\hat{\psi}_r^{(3)}$, a part of the torque is shifted to vector space 3 as defined by (7).

Step 2: Vector space 1 is demagnetized after the “Step 1” by reducing $i_s^{d(1)}$ while keeping $i_s^{d(3)}$ constant. It must be noted

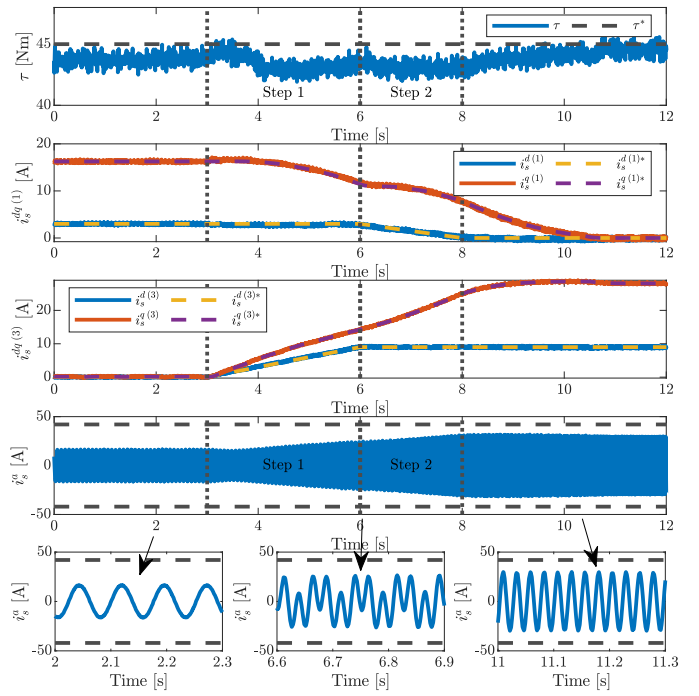


Fig. 8. Synchronous 1 \rightarrow 3 MPT technique using proposed RFPT.

that due to the electrical time constant of each vector space, the $\hat{\psi}_r^{(1)}$ does not immediately reduce to zero. Thus, the torque transition is not completed until the $\hat{\psi}_r^{(1)} \approx 0$. These dynamics of pole transition can be improved by implementing a simple $\hat{\psi}_r^{(1)}$ controller. However, it is out of the scope of this paper.

During the MPT, the total torque is distributed among vector spaces 1 and 3 as a function of $\psi_r^{(\nu)}$ given by (7). This expression ensures that the $\omega_{sl}^{(\nu)}$ of both vector spaces are synchronized (as given by (6)) resulting in a smooth transition from 1 pole pair to 3 pole pair configuration. Due to this synchronization between the vector spaces, the beat oscillations that were observed with the earlier proposed asynchronous control method are eliminated. Furthermore, by optimizing the alignment of current vectors of each vector space as described in section IV-A of [3], the stator current peaks are minimized, which can be observed during the pole transition. This reduction in the stator current peaks helps increase the margin between the converter's over-current limit. During the whole procedure, the $\hat{\omega}_s^{(\nu)}$ is defined by (11). Before “Step 1” and after “Step 2”, the $\hat{\omega}_s^{(\nu)}$ of each vector space is solely dependent on the vector space 1 and vector space 3, respectively. However, during the pole transition i.e. measurements between “Step 1” and “Step 2”, the $\hat{\omega}_s^{(\nu)}$ is constructed by combining the reference frame of vector spaces 1 and 3 based on their magnetizing levels. This makes both flux observers functional even when the corresponding vector space is not magnetized.

VI. CONCLUSION

This paper proposes an improved magnetic pole-pair transition (MPT) technique for a phase-pole modulating induc-

tion machine (PPMIM). During the pole transition stage, the torque is distributed between two pole configurations in such a way that the normalized frequency of each vector space stays synchronized. This is achieved by introducing smooth reference frame transition (SRFT) between the vector spaces of corresponding pole configurations. Due to this feature, the beat oscillations that are introduced in the output torque due to inter-plane cross-coupling (IPXC) are avoided, resulting in a ripple free pole-pair transition (RFPT). This MPT enables any PPMIM to have extended torque-speed characteristics, acting as a virtual gearbox. Furthermore, the performance of the PPMIM during a pole transition can be improved by optimizing the peaks of a given resultant vector of the electrical machine. In this paper, the peak optimization of the stator current is demonstrated to increase the margin between the stator current and the converter's over-current limit. All these features of the proposed RFPT based on an improved SRFT method are evaluated on a 9-phase induction machine (IM) in a laboratory and lay a solid foundation for the development of an optimal phase-pole modulation for a PPMIM.

REFERENCES

- [1] F. Barrero and M. J. Duran, "Recent advances in the design, modeling, and control of multiphase machines—part I," *IEEE Transactions on Industrial Electronics*, vol. 63, no. 1, pp. 449–458, 2016. [Online]. Available: <https://ieeexplore.ieee.org/document/7128683>
- [2] M. J. Duran and F. Barrero, "Recent advances in the design, modeling, and control of multiphase machines—part II," *IEEE Transactions on Industrial Electronics*, vol. 63, no. 1, pp. 459–468, 2016. [Online]. Available: <https://ieeexplore.ieee.org/document/7130602>
- [3] O. Ikram ul Haq, Y. Wu, L. Peretti, S. G. Bosga, and R. S. Kanchan, "Generalized harmonic injection strategy for multiphase induction machine control," *IEEE Transactions on Energy Conversion*, pp. 1–10, 2023.
- [4] A. Tani, M. Mengoni, L. Zarri, G. Serra, and D. Casadei, "Control of multiphase induction motors with an odd number of phases under open-circuit phase faults," *IEEE Transactions on Power Electronics*, vol. 27, no. 2, pp. 565–577, 2012. [Online]. Available: <https://ieeexplore.ieee.org/document/5744128>
- [5] E. Sayed, M. Abdalmagid, G. Pietrini, N.-M. Sa'adeh, A. D. Callegaro, C. Goldstein, and A. Emadi, "Review of electric machines in more-/hybrid-/turbo-electric aircraft," *IEEE Transactions on Transportation Electrification*, vol. 7, no. 4, pp. 2976–3005, 2021. [Online]. Available: <https://ieeexplore.ieee.org/document/9455401>
- [6] K. Nounou, J. F. Charpentier, K. Marouani, M. Benbouzid, and A. Kheloui, "Emulation of an electric naval propulsion system based on a multiphase machine under healthy and faulty operating conditions," *IEEE Transactions on Vehicular Technology*, vol. 67, no. 8, pp. 6895–6905, 2018. [Online]. Available: <https://ieeexplore.ieee.org/document/8356133>
- [7] J. Wang, R. Qu, and Y. Liu, "Comparison study of superconducting generators with multiphase armature windings for large-scale direct-drive wind turbines," *IEEE Transactions on Applied Superconductivity*, vol. 23, no. 3, pp. 5201005–5201005, 2013. [Online]. Available: <https://ieeexplore.ieee.org/document/6415250>
- [8] E. Libbos, E. Krause, A. Banerjee, and P. T. Krein, "Inverter design considerations for variable-pole induction machines in electric vehicles," *IEEE Transactions on Power Electronics*, vol. 37, no. 11, pp. 13554–13565, 2022. [Online]. Available: <https://ieeexplore.ieee.org/document/9779946>
- [9] O. Ikram ul Haq, L. Peretti, S. G. Bosga, and R. S. Kanchan, "Online Winding Reconfiguration of a Multiphase Stator," in *Power Electronics & Drive Systems (PEDS)*. Montreal, Canada: IEEE, Aug. 2023.
- [10] Y. Wu, G. F. Olson, and L. Peretti, "Pole-transition control of variable-pole machines using harmonic-plane decomposition," *IEEE Transactions on Industrial Electronics*, vol. 70, no. 8, pp. 7753–7760, 2023.
- [11] E. Libbos, B. Ku, S. Agrawal, S. Tungare, A. Banerjee, and P. T. Krein, "Variable-Pole Induction Machine Drive for Electric Vehicles," in *2019 IEEE International Electric Machines & Drives Conference (IEMDC)*. San Diego, CA, USA: IEEE, May 2019, pp. 515–522. [Online]. Available: <https://ieeexplore.ieee.org/document/8785212/>
- [12] S. Runde, A. Baumgardt, O. Moros, B. Rubey, and D. Gerling, "ISCAD — Design, control and car integration of a 48 volt high performance drive," *Trans. Electr. Mach. Syst.*, vol. 3, no. 2, pp. 117–123, Jun. 2019. [Online]. Available: <https://ieeexplore.ieee.org/document/8766933/>
- [13] O. Wallmark, K. Bitsi, and S. G. Bosga, "A Transient Model of WICSC and ISCAD Machines Based on Permeance Networks," in *2020 International Conference on Electrical Machines (ICEM)*. Gothenburg, Sweden: IEEE, Aug. 2020, pp. 2048–2054. [Online]. Available: <https://ieeexplore.ieee.org/document/9270733/>
- [14] M. Slunjski, O. Dordevic, M. Jones, and E. Levi, "Symmetrical/Asymmetrical Winding Reconfiguration in Multiphase Machines," *IEEE Access*, vol. 8, pp. 12835–12844, 2020. [Online]. Available: <https://ieeexplore.ieee.org/document/8955871/>
- [15] A. G. Yepes, J. Doval-Gandoy, F. Baneira, D. Perez-Estevez, and O. Lopez, "Current Harmonic Compensation for n - Phase Machines With Asymmetrical Winding Arrangement and Different Neutral Configurations," *IEEE Trans. on Ind. Applicat.*, vol. 53, no. 6, pp. 5426–5439, Nov. 2017. [Online]. Available: <http://ieeexplore.ieee.org/document/7964705/>
- [16] S. V. S. P. K. Ch, V. Sonti, and S. Jain, "Gradual electronic pole changing technique to minimize the circulating currents during pole/mode transition in induction motor drive," *IEEE Transactions on Industry Applications*, vol. 59, no. 1, pp. 959–969, 2023. [Online]. Available: <https://ieeexplore.ieee.org/document/9896150>
- [17] H. Jia, G. Yang, and J. Yang, "Electronic pole-changing strategy with cosine-response for multiphase induction motor based on pr controller," *Journal of Electrical Engineering & Technology*, vol. 17, no. 1, pp. 261–269, 2022. [Online]. Available: <https://doi.org/10.1007/s42835-021-00837-y>
- [18] B. P. Reddy, A. Iqbal, S. Rahman, M. Meraj, and S. Keerthipati, "Dynamic modeling and control of pole-phase modulation-based multiphase induction motor drives," *IEEE Journal of Emerging and Selected Topics in Power Electronics*, vol. 10, no. 3, pp. 3383–3394, 2022.
- [19] I. Balan, A.-I. Timofte, V. Horga, and A. Salceanu, "Simulation and control of a nine phase induction machine with pole-phase modulation used in propulsion system for electric vehicles," in *2023 International Conference on Electromechanical and Energy Systems (SIEMEN)*, 2023, pp. 1–8.
- [20] M. Jecmenica, B. Brkovic, E. Levi, and Z. Lazarevic, "Interplane cross-saturation in multiphase machines," *IET Electric Power Applications*, vol. 13, no. 11, pp. 1812–1822, Nov. 2019. [Online]. Available: <https://onlinelibrary.wiley.com/doi/10.1049/iet-epa.2018.5546>
- [21] Y. Zhao and T. Lipo, "Modeling and control of a multi-phase induction machine with structural unbalance," *IEEE Trans. On energy Conversion*, vol. 11, no. 3, pp. 570–577, Sep. 1996. [Online]. Available: <http://ieeexplore.ieee.org/document/537009/>
- [22] L. Harnefors, S. E. Saarakkala, and M. Hinkkanen, "Speed control of electrical drives using classical control methods," *IEEE Transactions on Industry Applications*, vol. 49, no. 2, pp. 889–898, 2013.
- [23] O. Ikram ul Haq, L. Peretti, and M. Hinkkanen, "Estimation of Equivalent Circuit Parameters of Multiphase Induction Machines by Exploitation of Space Harmonic Relations," in *International Electric Machines & Drives Conference (IEMDC)*. San Francisco, California: IEEE, May 2023.